W. Afzal, J. Prausnitz

FOUR METHODS FOR MEASURING THE SOLUBILITIES OF GASES AND VAPORS IN LIQUIDS AND POLYMERS

Introduction. Solubilities of gases and vapors at low or moderate pressures and ordinary temperatures have attracted attention from physical chemists and chemical engineers for more than a century. Experimental methods for measuring such solubilities have been reviewed in numerous publications; particularly noteworthy are the reviews by Weissberger and Rossiter [1] and by Battino and co-workers [2, 3]. The IUPAC Commission on Thermodynamics published a multi-volume series on Experimental Thermodynamics; in that series, Volume VII: Measurement of the Thermodynamic Properties of Multiple Phases [4] presents a valuable state-of-the-art summary. Other useful studies include discussions by Richon [5, 6], Raal and Mühlbauer [7], Malanowski [8, 9], Hala et al. [10], and Dohrn and Brunner [11].

This review is limited to four relatively new methods that, in our experience, are particularly useful for informing chemical process design; in a sense, it is a somewhat personal review because it emphasizes studies performed at Berkeley. No attempt is made here to provide a global review.

Each of the four methods has particular advantages and disadvantages, depending on the nature of the solute and that of the solvent, and on operating conditions such as pressure.

Accurate determination of solubility is not easy, especially if the solubility is very small. However, with care and attention to detail, the methods reviewed here can provide solubilities with uncertainties of no more than about 3 or at most 5 percent. Only the synthetic-volumetric method is applicable for those systems where the gas solubility at ordinary pressures is very small.

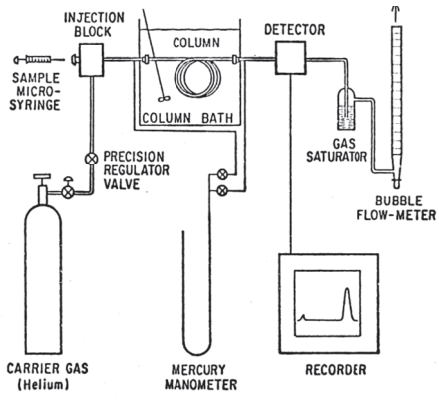

Fig. 1. Gas-liquid chromatograph for solubility measurements (from [13])

The Chromatographic method. Gas-liquid chromatography (GLC) provides a useful technique for determination of infinite-dilution activity coefficients (or Henry's constants) of vapors in non-volatile solvents. The technique is well-established for studying molecular interactions of volatile liquids with polymers [12–16] or with ionic liquids [17].

Fig. 1 [16] shows the essential elements of gas-liquid chromatography. For solubility measurements we require a commercially available gas-liquid chromatograph and custom-made columns coated with the liquid solvent (stationary phase). For the mobile phase, we require an inert and insoluble carrier gas like helium. The solute is injected into the column immediately at the en-

Waheed Afzal — post-doc, university of California, Berkeley, USA; e-mail: waheed.afzal@gmail.com
John Prausnitz — professor, university of California, Berkeley, USA;
e-mail: prausnit@cchem.berkeley.edu

trance to the column. We also require a flow meter to measure the flow rate of the carrier gas.

The position of the measured chromatographic peak provides the retention time (t_r), that is given by the distance between the time of injection and that of the peak maximum on the chromatogram. This retention time can be converted to retention volume by multiplying with the average volumetric flow rate of the carrier gas. The retention volume follows from two distinct contributions: one from the empty volume inside the column (holdup) and the other, from molecular interactions of the sample with the stationary phase (elution). The holdup of the column can be determined by injecting a tracer gas (e. g. hydrogen) that shows no interaction with the stationary phase.

Infinite-dilution activity coefficients and Henry's constants are calculated using an equation derived by Cruickshank et al. [18]:

$$\ln \gamma_i^{\infty} = \ln \frac{n_L RT}{V_{N,i} P_i^0} - \frac{(B_{ii} - V_i^0) P_i^0}{RT} + \frac{(2B_{ij} - \overline{V}_i^{\infty}) J P_2}{RT}, \tag{1}$$

where γ_i^{∞} is the activity coefficient of solute i at infinite dilution in the stationary phase; P_i^0 is the vapor pressure of the pure liquid solute; n_L is the number of moles of liquid in the column; B_{ij} is the second virial coefficient for the i—j interaction where i is solute and j is solvent; v_i^0 is the molar volume of i and $\overline{V}_i^{\infty}$ is the partial molar volume of i in the solute; V_i^0 is liquid molar volume; J is corrects for pressure drop according to Eq. (4); P_2 is the outlet pressure of the column. The standardized retention volume $V_{N,i}$ is calculated from Eq. (3).

Eq. (1) contains two correction terms, one to account for the non-ideality of the mobile gas phase and the other for pressure drop. However, in most cases, the contributions of the correction terms are small [13–16]. In those cases, Eq. (1) simplifies to

$$\gamma_i^{\infty} = \frac{n_L RT}{V_{N,i} P_i^0}, \tag{2}$$

where

$$V_{N,i} = J(t_r - t_h) U_0 \frac{T}{T_f}, \tag{3}$$

where t_r is the retention time of the solute; t_h is the hold-up time of the tracer gas (hydrogen); U_0 is the flow rate obtained from a flow meter connected to the outlet of the thermal-conductivity detector of the gas chromatograph; T is the column temperature; T_f is the flow-meter temperature assumed to be ambient temperature; $U_0(T/T_f) = U$ is the average volume flow rate inside the column. Factor J accounts for the pressure drop along the column given by [13–16]:

$$J = \frac{3}{2} \frac{(P_1/P_2)^2 - 1}{(P_1/P_2)^3 - 1}, \tag{4}$$

where P_1 and P_2 are the inlet and the outlet pressure of the column, respectively.

Henry's constant H_i is related to γ_i^{∞} by

$$H_i = \gamma_i^{\infty} P_i^0. \tag{5}$$

Two types of columns can be used: packed-bed and open-tube (capillary) columns. Packed columns are prepared by dissolving a weighed amount of the liquid solvent or polymer

dissolved in a highly volatile solvent. A weighed amount of an inert support material (e. g. Fluoropak or Chromsorb W or G, acid washed, DMCS treated, particle size 60/80, 80/100 or 100/120 mesh) is stirred into the solution. The mixture is then placed in a rotary vacuum evaporator to remove the volatile solvent, yielding a solid support coated with the liquid solvent or polymer. The coated support is then packed into a previously washed and dried stainless-steel or glass tube [13–16].

Capillary columns are coated with the liquid solvent or polymer by passing a solution of the liquid solvent or polymer dissolved in a highly volatile solvent through the previously cleaned capillary tubing and evaporating the volatile solvent. A high-precision weighing balance is used to determine the quantity of stationary phase coated on the inner wall of the capillary column [13, 14].

Both types of column must be conditioned, i. e., dried in a vacuum oven to achieve constant mass. The column is then installed in the GC oven with a low flow of helium for a few hours. The mass of coated solvent should be checked after conditioning. Measurements should be carried out promptly after column preparation to avoid aging effects [13–16].

Table 1

Comparison of open capillary and packed-bed GLC columns (from [19–22])

	Packed-Bed	Capillary
Length, m	1–5	5–60
I.D., mm	2–5	0.10–0.53
Plates per length, m^{-1}	1000	5000
Total Plates	5000	300000
Flow rate, mL/min	10–60	0.5–15
Permeability, 10^7 cm^2	1–10	10–1000
Liquid film thickness, μm	5–10	0.1–2
Capacity	High	Low
Resolution	Low	High
Pressure drop	High	Low

The major difference between packed and capillary columns is β, the ratio of volume of mobile phase to volume of stationary phase ($\beta = V_G/V_L$). In capillary columns, the number of theoretical plates per unit length is about 2 to 4 times larger than that for packed columns. Capillary columns have very low pressure drop and have low space requirements, making them suitable for long columns. Capillary columns are manufactured in 30 m lengths whereas packed columns are shorter than 5 m. A large β gives an important advantage to capillary columns that can provide larger separation of t_r and t_h; that separation should be large for accurate results. Several authors [19–22] have presented a detailed comparison of both types of column. Table 1 gives a brief summary [22].

Determination of hold-up volume of each column is a critical step, as indicated by Eq. (3). Fig. 2 shows hold-up volumes for four different columns coated with ionic liquids. One capillary column and two packed columns are coated with ionic liquid 1-ethyl-3-methylimidazolium acetate (Fig. 2, *a*) [14] and one capillary column is coated with ionic liquid 1-butyl-3-methylimidazolium hydrogensulfate (Fig. 2, *b*) [14]. Because column holdup depends on helium flow rate, measurements must be made in the range of the "optimum" flow rates.

The flow rate of the carrier gas should be such that the experimental data are independent of the flow rate. Earlier studies [14, 23] indicated that the best flow rate for a capillary column is in the range 4–6 mL/min as shown in Fig. 3. The optimum flow rate for a packed column is 5–10 ml/min.

The sample size should be as small as possible but must be sufficiently large to provide a clear signal in the detector. The optimum solute sample size is 0.1–2 μL.

Loading of the liquid solvent in the column should be high enough to avoid adsorption [13, 16]. For packed columns, adsorption is insignificant at a loading greater than 15 mass % [13, 14, 16].

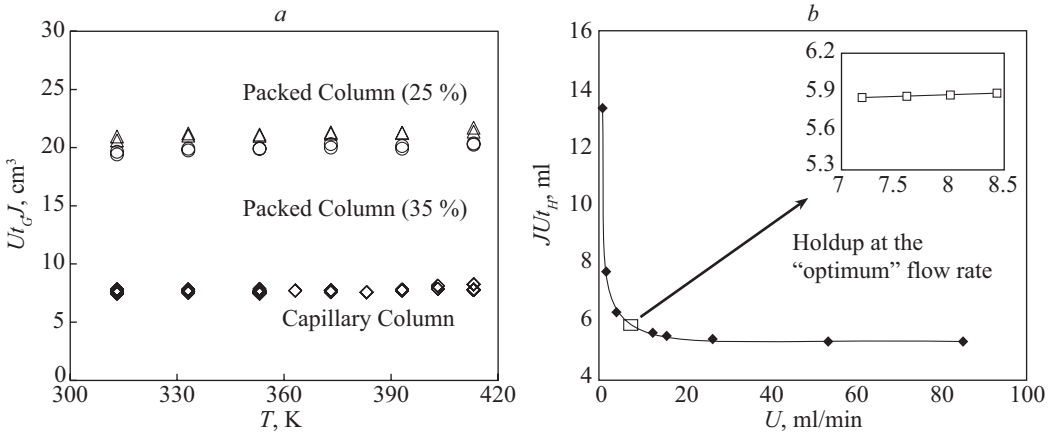

Fig. 2. Holdup volume at 313 K, Ut_GJ where U is helium flow rate in the column, t_G is hydrogen retention time and J is the pressure-drop correction factor, for four different columns coated with ionic liquid 1-ethyl-3-methylimidazolium acetate [14] (*a*) and capillary column coated with ionic liquid 1-butyl-3-methylimidazolium hydrogensulfate [23] (*b*): column holdup should be determined at the optimum flow rate at each temperature

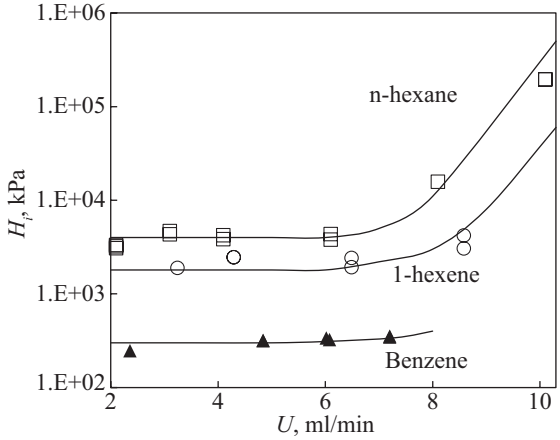

Fig. 3. Influence of flow rate U on Henry's constant H_i for the capillary column for three moderately soluble vapors in ionic liquid 1-ethyl-3-methylimidazolium acetate at 313 K: experiments for solubility should be conducted in the flat plateau region; the lines are to guide the eye (from [14])

Results. Henry's constants for several solutes can be obtained simultaneously by injecting all solutes at the same time. Fig. 4 presents Henry's constants for six solutes measured simultaneously with a capillary column.

At Berkeley, we measured solubilities of several volatile solutes in different polymers [12, 13, 15–17] and in different ionic liquids [14, 23] using both capillary and packed columns. Fig. 5 shows that results from a capillary column agree well with those from a packed column [12–17, 23].

Inert-gas stripping method. The inert-gas stripping (IGS) method is based on stripping a very small quantity of solute from the solvent with an inert gas; it is also known as the exponential dilutor technique. Leroi et al. [24] were the first to describe the pertinent experimental procedures and data reduction. However, over the years, several studies [25–31] have improved the accuracy of the results and extended the technique to corrosive and viscous systems. These studies have improved the material of construction and design

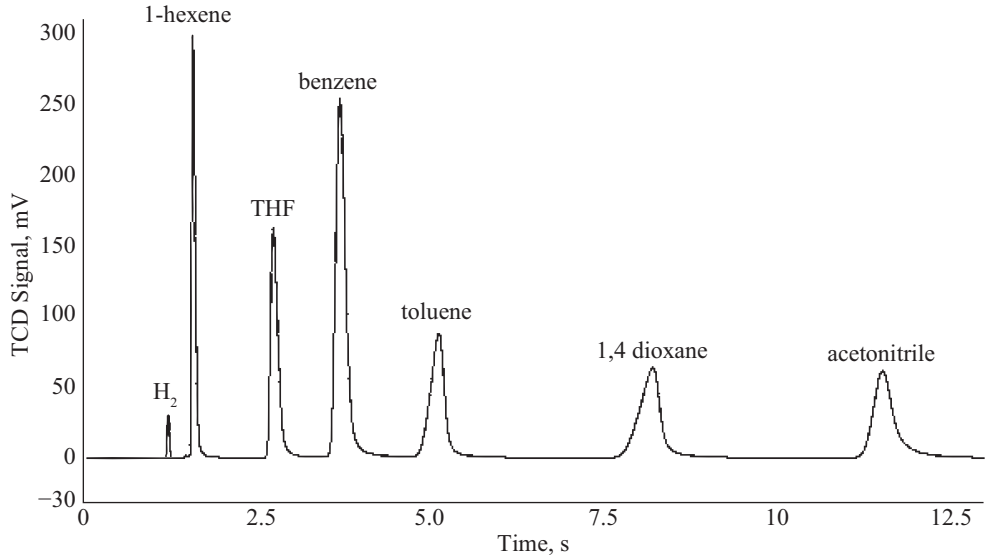

Fig. 4. Simultaneous measurement of Henry's constants for six solutes in 1-ethyl-3-methylimidazolium acetate at 333 K:
the data are from a capillary column [14]; see also Table 2

Table 2

The data for Fig. 4

	1-Hexene	THF	Benzene	Toluene	1,4-Dioxane	Acetonitrile
H, kPa (single)	3181	290	161	101	54	37
H, kPa (mixture)	4453	290	158	97	52	37

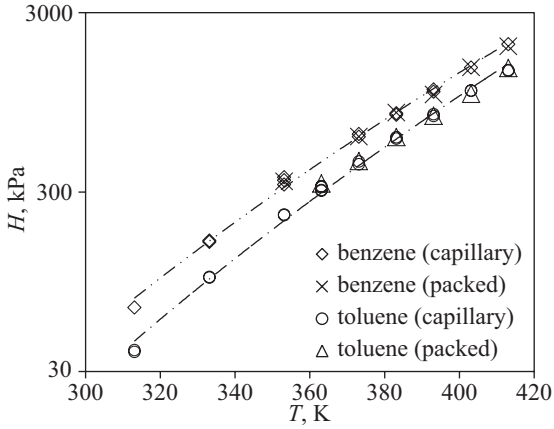

Fig. 5. Henry's constants for benzene and toluene in 1-ethyl-3-methylimidazolium acetate obtained from gas chromatography with different columns:
the lines are to guide the eye (from [14])

of the equilibrium cell, and the distribution of the inert gas to achieve better mass transfer between the solvent and the stripping-gas bubbles [24–30].

Fig. 6 shows the essential elements of an IGS apparatus built at Berkeley [32]. The apparatus consists of a glass vessel containing a magnetic stirrer and two vertical baffles to facilitate mixing. The glass vessel houses 10 stainless-steel 100 μm I.D. capillaries connected

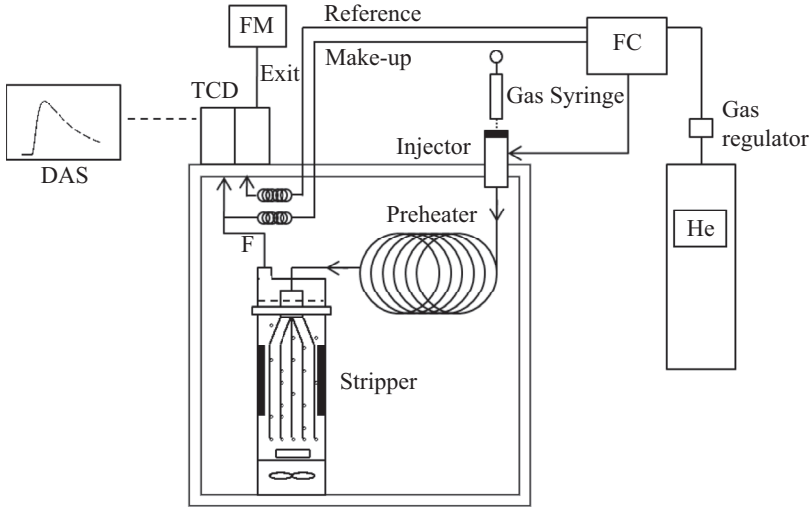

Fig. 6. Experimental apparatus for using the inert-gas stripping method: the stripper and preheater are installed in the oven of a commercial GC; FM is the flow meter; FC is the flow controller; TCD is the thermal-conductivity detector (from [32])

to a supply of inert gas (helium). These capillaries bubble helium through the liquid. The cap of the stripper prevents liquid entrainment in the exiting gas.

The stripper is placed inside the column oven of a commercial gas chromatograph (GC) with a thermal-conductivity detector (TCD). The temperature of the oven is controlled with an air bath. The temperature, pressure, and flow rate are set and the detector signal is recorded using the operating software provided with the GC. A calibrated gas-flow meter is required to determine the flow rate of inert gas at the exit of the detector. A magnetic stirrer agitates the liquid inside the stripper.

The inlet of the stripper is connected to the injector of the GC. A 2-m-long coil of tube serves as a heat exchanger to allow helium to attain the desired temperature. The injector is heated about 10 K above the desired temperature. The exit of the stripper is connected to the TCD through a small tube. A gas syringe is used to inject 2 to 5 mL of solute gas into the injector. A continuous and constant flow of helium is set. The detector is set at a high temperature to avoid condensation [31]. The apparatus shown in Fig. 6 does not require sampling.

Earlier studies [25–31] have described data reduction. Following Duhem and Vidal [31], Henry's constant Hi is given by

$$H_i = m\frac{n_j RT}{F - mV_g}, \tag{6}$$

where m is the slope of the "stripping" curve (explained later), Henry's constant H_i is for gas i; t is time and s_i is any property of the gas phase directly proportional to the gas-phase concentration; n_j is the number of moles of solvent in the stripper; R is the gas constant; T is temperature; F is the flow rate of inert gas in the stripper and V_g is the vapor-space volume above the liquid in the stripper. Eq. (7) defines slope m. Because the concentration of solute in the solvent is decreasing with time, slope m is always negative. In our studies [32], we determined slope m from the TCD signal as shown in Fig. 7. Because sparingly-soluble

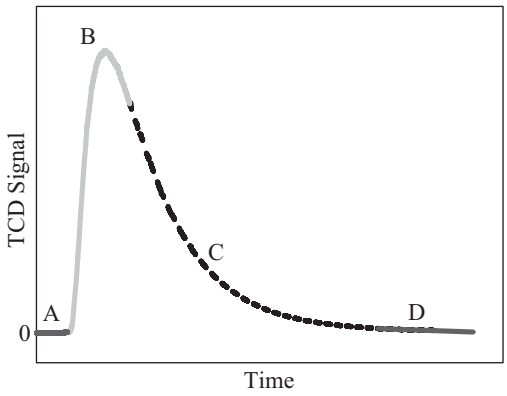

Fig. 7. Typical stripping profile for a gas-liquid system using helium for stripping: segment A shows the stable baseline; B shows injection of solute-gas; segment C (dashed line) is the exponential stripping curve used to determine slope m; line D shows the final part of the stripping curve as $s_i \to 0$ (from [32])

gases leave the liquid rapidly, earlier methods based on sampling and analysis could not measure solubilities of sparingly-soluble gases in liquids [33].

The liquid solvent is placed into the stripper in such a way that vapor space V_g in the stripper is minimized (see Eq. (6)) [31, 34]. After placing the stripper inside the oven of the GC and connecting it with the GC injector, helium flows at a constant rate while maintaining good agitation in the stripper. The exit line of the stripper is connected to the main line of the GC detector. After the detector's baseline is stable ($s_i = 0$), the solute gas is injected into the stripper through the GC injector. For sparingly-soluble gases like oxygen and nitrogen, about 5 ml of gas is sufficient; however, for more soluble gases like carbon dioxide, 1–2 mL is enough. Helium and the solute gas pass through the solvent. The solubility of the solute gas is substantially higher than that of helium. The solute makes a very dilute solution. The constant flow of helium continuously strips the solute away; the exit gas passes through the TCD, providing a real-time profile of the gas-phase composition in terms of signal s_i as a function of time, as shown in Fig. 7. The detector must operate in the linear range, usually 3 to 5 orders of magnitude higher than the detection limit. Before injecting solute gas into the stripping cell through the GC injector, the baseline of the detector should be set at zero. Agitation should ensure equilibrium between helium bubbles and the liquid phase. The small vapor space inside the stripper must be carefully calculated using the known volume of the stripper and the mass and density of the liquid [32].

At constant helium flow rate, detector signal s_i (or composition of solute in exiting-stripping gas) decreases exponentially with time t:

$$s_i = p \exp(mt). \tag{7}$$

Here, m is the slope of the stripping curve and p is an insignificant constant.

Fig. 7 [32] shows a typical stripping curve and a procedure to obtain slope m of the pertinent segment of the curve. Segment A shows a stable baseline signal at $s_i = 0$; segment B shows a sharp rise of the signal due to the injection of solute; segments C and D show an exponential decrease in signal due to depletion and finally, complete removal of solute from the solvent. Slope m is determined from the data given in segment C, shown as a dotted line. Upon fitting the data, a high coefficient of regression ($R^2 \geqslant 0.999$) provides an indication of reliable measurements [32].

For gases or vapors having high solubilities, experimental uncertainties are small. However, for gases that have very low solubilities ($x_i \sim 10^{-4}$), the uncertainty depends upon several factors related to the design and operation of the stripper. It is essential to achieve

equilibrium between stripping-gas bubbles leaving the liquid surface and the bulk liquid. When using viscous solvents (viscosity > 10 cP) and/or low-soluble gases, the experiment should be repeated several times at slightly different flow rates.

Henry's constant must be independent of flow rate while working in the optimized flow-rate range. An unusually high Henry's constant and/or a poor coefficient of regression ($R^2 < 0.99$) indicate an unsteady flow rate or failure to attain equilibrium inside the stripper [32].

Fig. 8 [32] shows the influence of flow rate on Henry's constant for air in n-dodecane at room temperature. Flow rates near 10 cm^3/min give best results for n-dodecane. Higher flow rates (> 15 ml/min) give experimental scatter. Lower flow rates (< 5 mL/min) are difficult to maintain and to measure accurately. For solvents with higher viscosity like ethylene glycol, the flow rate should be 6–8 cm^3/min [32].

Fig. 9 [32] shows the influence of agitation on Henry's constant for oxygen in n-dodecane at room temperature. Agitation varies from 100 to 1500 rpm. Each experiment to obtain Henry's constants is conducted at least twice to note data scatter. The data show appreciable scatter at very low agitation. Stirring above 500 rpm gives good results [32].

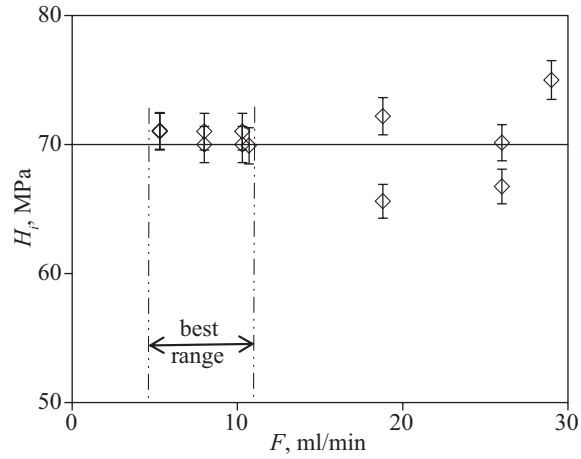

Fig. 8. Influence of flow rate on Henry's constant for air in n-dodecane at 300 K:

the best flow rate is in the range 5–10 cm^3/min; the error bars are ±3 %, H_i = 69 MPa (from [32])

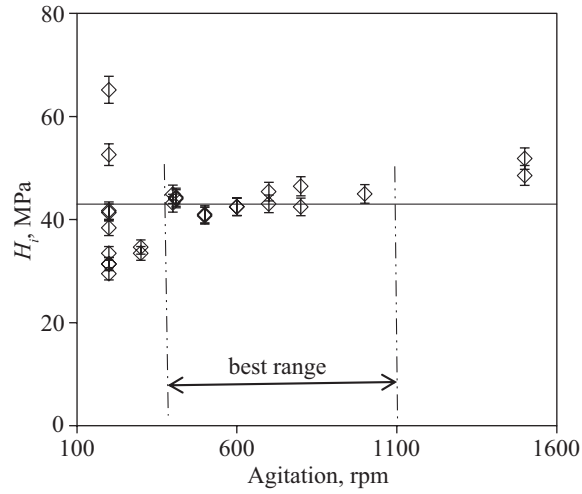

Fig. 9. Influence of agitation on Henry's constant for O_2 in n-dodecane at 300 K:

the best agitation is in the range 500–1000 rpm; the error bars are ±3 %, H_i = 44 MPa (from [32])

The length of the stripper is more important than its diameter. The size of the stripper is determined using trial-and-error [25–32]. The length should provide sufficient residence time for helium bubbles to achieve equilibrium in the well-mixed liquid in the stripper.

Results. From IGS measurements, Table 3 [32] gives Henry's constants for krypton, oxygen, and nitrogen in ionic liquid 1-butyl, 3-hydrogen-imidazolium acetate. The data obtained using the IGS method agree well with those obtained from the synthetic-volumetric method, described later.

Table 3

Comparison of Henry's constants (H_i) for three gases in ionic liquid 1-butyl, 3-hydrogen-imidazolium acetate using the inert-gas stripping method with those using the synthetic-volumetric method (from [32])

Solute	T, K	H_i, MPa	RSD*, %
IGS method			
Kr	308	40.0	6
O_2	307	115	6
O_2	310	120	7
N_2	308	180	8
Synthetic-volumetric method			
Kr	303	41.9	3
Kr	313	43.0	2
Kr	323	44.4	1
Kr	333	45.0	2
O_2	303	121	3
O_2	308	118	3
O_2	313	123	2
N_2	304	174	2
N_2	313	170	3

* RSD — relative standard deviation; the average is taken from a minimum of 3 measurements.

Gravimetric quartz-spring method. Absorption of a gas in a liquid causes an increase in the liquid's mass. The gravimetric quartz-spring method provides a high-sensitivity micro-balance inside a closed environment. Several studies report solubilities of vapors in polymers or ionic liquids using this method [35–40]. The increase in mass must be sufficiently large for accurate measurement of the quart-spring displacement. Therefore, this method is not useful for measuring solubilities of sparingly-soluble gases [39].

Fig. 10 [35] gives a schematic diagram of a glass-apparatus for the gravimetric quartz-spring method. The apparatus consists of a sample-pan (typically aluminum) that is suspended by a delicate quartz spring inside a transparent chamber. The spring length is carefully determined using a cathetometer. The temperature of the chamber is controlled using a constant-temperature bath. Sensors measure temperature and pressure inside the chamber. A calibration relates quartz-spring length to mass [35–40].

For measuring solubilities of vapors, condensation is avoided by using pressures inside the chamber below the saturation pressure of the solute. For a typical experiment, a small quantity of a non-volatile liquid or polymer is placed into the sample-pan. The chamber is evacuated to remove air and traces of volatile matter. Solute vapor is introduced into the chamber. The system is allowed sufficient time to reach equilibrium, typically several hours.

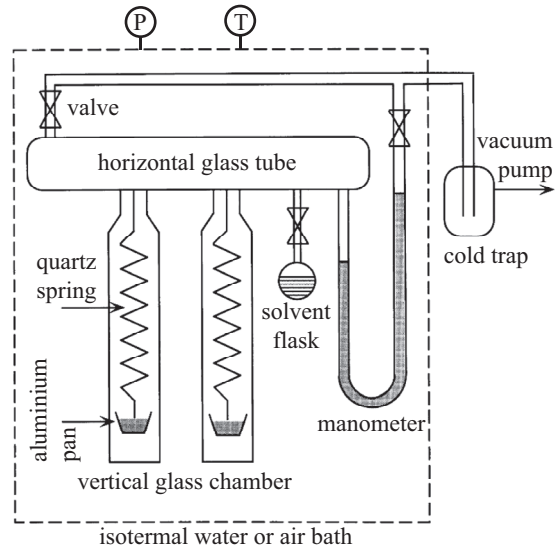

Fig. 10. Experimental apparatus for the gravimetric quartz-spring method to measure the solubility of a vapor in a non-volatile solvent (from [35])

The change in the length of the spring provides the change in mass of the liquid sample due to absorption of solute. Addition of more solute vapor causes further increase in the length of the spring due to rise in pressure. These data establish an isothermal plot of solubility versus pressure.

The calibration curve for the spring (mass versus length) is usually linear and temperature-independent. At normal pressures, buoyancy effects are usually negligible.

To increase the rate of data production, and to determine the impact of buoyancy, it is desired to use two (or more) quartz springs, each with a sample pane, in the equilibrium chamber, as shown in Fig. 10.

Results. Fig. 11 [36] shows the solubility of water vapor in three different polymers exhibiting hydrophobic or hydrophilic character. Fig. 12 shows the solubility of carbon dioxide in ionic liquid 1-butyl-3-methylimidazolium hexafluorophosphate [39].

The synthetic-volumetric method. This method requires an equilibrium cell with temperature and pressure sensors and an assembly for gas and liquid loading. Once solute and solvent are placed into the equilibrium cell, a suitable stirring system provides equilibration of phases. Equilibrium phase compositions can be determined by sampling and analysis, by *in situ* analysis, by PVT data, or by a combination [4–12, 41–44].

Fig. 13 [41–44] shows the essential elements of an apparatus for using the synthetic-volumetric method with an isochoric equilibrium cell.

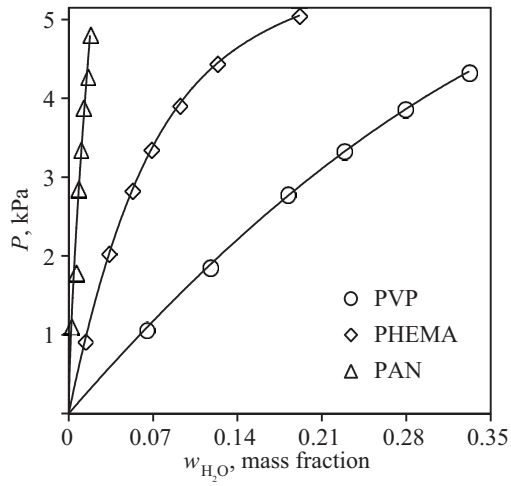

Fig. 11. Solubility of water vapor in three polymers:

poly (acrylonitrile) or PAN, poly 2-hydroxyethylmethacrylate or PHEMA, and poly n-vinyl-2-pyrrolidone or PVP at 308 K (from [36])

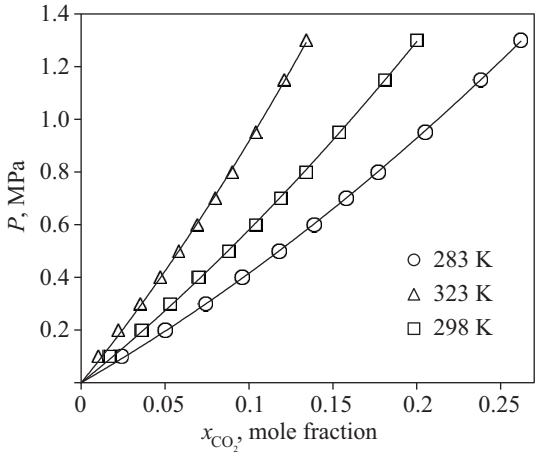

Fig. 12. Solubility of carbon dioxide in ionic liquid 1-butyl-3-methylimidazolium hexafluorophosphate (from [39])

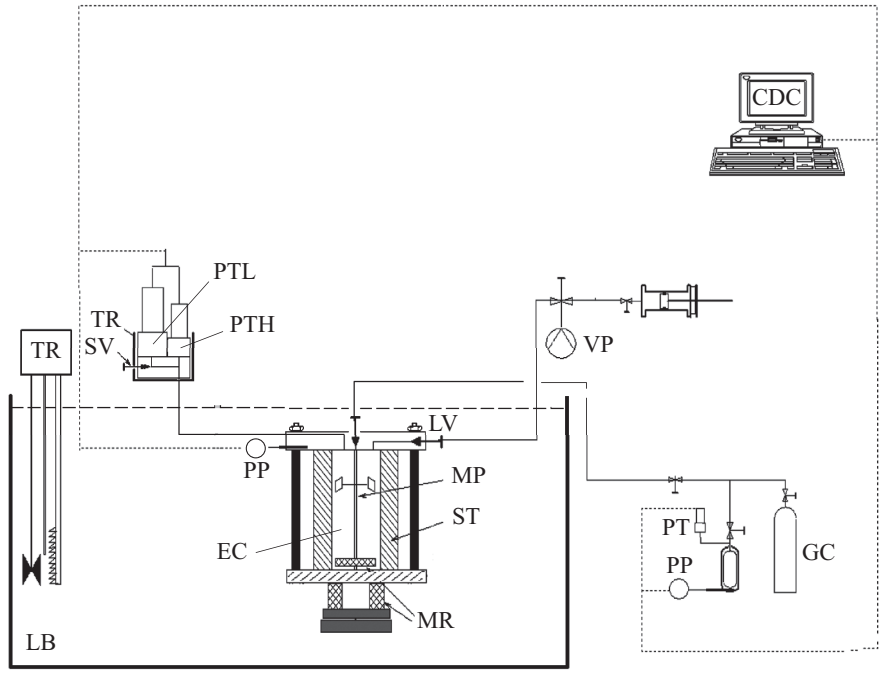

Fig. 13. Experimental apparatus for the synthetic-volumetric method for measuring solubilities of sparingly-soluble gases in liquids (from [41]):

CDC — central desktop computer; EC — equilibrium cell; GC — gas cylinder (reservoir); LB — liquid bath; LV — loading valve; MR/MP — magnetic rod/propeller; PP — temperature sensors; PT — pressure transducer; ST — stainless-steel tube; TR — temperature regulator; VP — vacuum pump

In the closed-system static technique, equilibrium is achieved using a single or double stirrer without circulation of either phase. It is advantageous to use a transparent cell for observing the mixture. The stirrers are either magnetically or mechanically coupled with an external motor. For advanced pressures (generally up to 20 MPa), we can use a transparent sapphire tube, held between stainless-steel or titanium flanges. For safety, a high-pressure rupture disc or pressure-relief valve is necessary [41–43].

For this method we used a procedure similar to that described earlier [41, 43, 44]; however, Fig. 13 shows a new version of the equilibrium cell. Required data are equilibrium temperature, pressure, volumes, and molar quantities placed into the equilibrium cell. These data are used to determine the composition of the liquid phase without sampling for composition [41, 44].

The synthetic method, based on total-pressure measurement, is particularly useful for obtaining the solubility of a single gas in a single liquid for a range of temperature and pressure. Table 4 [44] presents advantages and limitations of this method.

Table 4

Summary of some common synthetic methods used for measuring gas solubilities (from [44])

Technique	Description	Remarks
Cell with visual observation [4–6].	A fixed or variable-volume cell possibly with visual observation (naked or assisted with spectroscopic means) is used to note appearance of liquid drops (dew point) or vapor bubbles (bubble point). The cell may be able to measure some physical properties in addition to temperature and pressure. The global composition of mixture is known, either from mass balance or from PVT properties.	The observed bubble/dew point data are not at, but very near the true values even with assisted instrumental-observations because observations are only possible once the effect (drop of liquid or bubble of vapor) occurs. The system should not be in the retrograde or critical region. For safety, high pressures (above 25 MPa) are not possible because the cell window may break. Cells made of glass can be used for moderate pressure studies.
Non-visual or blind cell [5, 46].	A fixed or variable-volume cell for measuring PTV properties can give isothermal P—V or isochoric P—T curves indicating transition from a one-phase mixture to a two-phase mixture. The global composition of the mixture loaded into the cell is determined either from weighing or from PVT properties.	Several materials of construction are available for high-pressure applications. Isothermal P—V methods are faster than isochoric P—T methods because hydraulic equilibrium is attained more rapidly than thermal equilibrium; heat transfer in thick walls is slow. The mixture should not be in the retrograde or critical region.
Total pressure method [47–49].	An equilibrium cell for measuring PTV properties for known molar quantities of fluids. It can be used to determine PTx data. The molar quantities are determined either from mass balance or from PVT properties.	The measurement technique is relatively rapid. $PTxy$ data can also be obtained using the Gibbs—Duham equation if a suitable thermodynamic model is available. This method is useful for measuring solubilities of gaseous mixtures in liquids if the vapor phase can be analyzed at equilibrium [44].

Summary of the experimental procedure.

1. The liquid is heated to about 373 K under vacuum for more than five hours to remove any volatile compounds and water.

2. The equilibrium cell and the loading lines are cleaned with ethanol, dried, and evacuated to eliminate air and ethanol used for cleaning.

3. Freshly degassed solvent is loaded into the equilibrium cell; mass of equilibrium cell before and after loading provides the mass of liquid.

4. The lid of the equilibrium cell is tightened carefully; o-rings are used to prevent leakage.

5. The liquid is heated to about 350 K and degassed for about a half hour to remove air. The equilibrium cell is weighed again to re-determine the mass of liquid in the cell.

6. The temperature of the equilibrium cell is set by immersing it in the pre-set temperature of the liquid bath.

7. The gas is loaded into the equilibrium cell from the gas-loading assembly. Pressure and temperature are measured before and after introducing gas into the equilibrium cell to determine the quantity of gas introduced.

8. The phases are equilibrated using a stirrer. The equilibrium pressure and temperature are recorded.

9. The temperature of the equilibrium cell is changed to determine solubility at a new temperature.

From mass balances, the liquid-phase composition is calculated using the equilibrium temperature, pressure and volume, and the quantities of gas and liquid loaded into the equilibrium cell [41–44]:

$$n_i^{T(EC)} = n_{i(\text{initial})}^{\text{GRes}} - n_{i(\text{final})}^{\text{GRes}} \tag{8}$$

and

$$n_i^T = n_i^V + n_i^L, \tag{9}$$

where n_i is number of moles of i; superscripts V and L represents equilibrium phases, superscript T stands for total, GRes is gas reservoir, and EC represents equilibrium cell. If temperature and pressure of the system are not high, n_i^V (moles of gas in vapor phase) can be expressed as

$$n_i^V = \frac{y_i V^V}{\sum y_{iv_i}}, \tag{10}$$

where y_i is the vapor-phase mole fraction; V^V is the volume of vapor phase and v_i is the molar volume of gas. For a single gas at normal temperature and low pressure, and for a non-volatile liquid, the vapor phase can be assumed pure, eliminating the need for vapor-phase composition ($y_i = 1$). Number of moles of liquid (n_j^T) is obtained from mass of the liquid placed into the equilibrium cell.

$$x_i = \frac{n_i^L}{n_i^L + n_j^T}, \tag{11}$$

where subscript j is liquid and x_i is gas solubility i. e. the mole fraction of solute in the liquid phase.

Results. Fig. 14 [41] presents solubility data for oxygen in ionic liquid 1-butyl-3-methylimidazolium tetrafluoroborate obtained from the volumetric-synthetic method. Comparison with solubility data reported by Jacquemin et al. [45] shows good agreement.

Table 3 [31] compares Henry's constants for krypton, oxygen and nitrogen in ionic liquid 1-butyl, 3-hydrogen-imidazolium acetate obtained from solubility data using the volumetric-synthetic method with those obtained from the IGS method. Agreement is good.

Conclusion. This brief review described four methods for obtaining solubilities of gases and vapors in liquids or polymers: gas-liquid chromatography, inert-gas stripping, gravimetric quartz-spring, and the synthetic-volumetric method.

For each method, we have shown the essential features of the experimental equipment constructed at Berkeley. Whenever possible, we compare solubility results obtained from different methods. We have indicated the applications and limitations of each method. It is not easy to obtain reliable solubility data, especially when the solubility is very small.

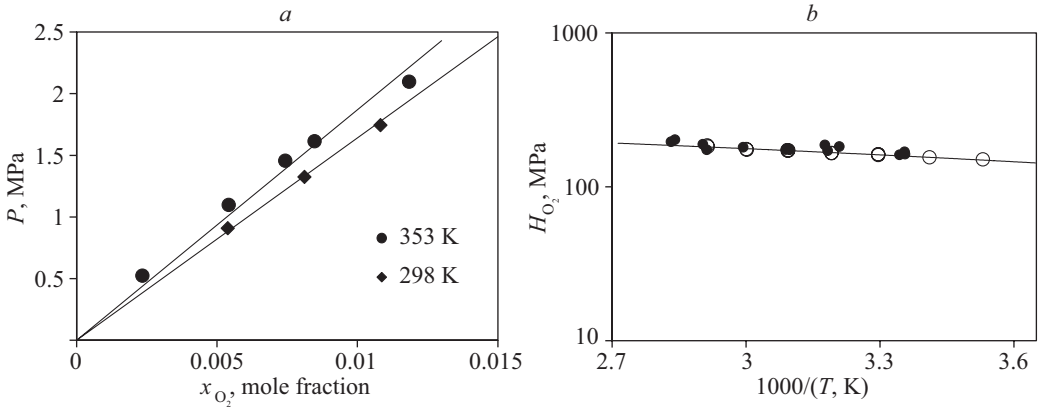

Fig. 14. Solubility of oxygen in ionic liquid 1-butyl-3-methylimidazolium tetrafluoroborate from the volumetric-synthetic method:

a — high-pressure solubility results from [41]; *b* — Henry's constants obtained from solubility data from [41] (solid markers) are compared with those from [45] (hollow markers)

However, with care and with meticulous attention to details, good results can be obtained. The synthetic-volumetric method is particularly useful for obtaining solubilities of sparingly-soluble gases in liquids.

* * *

This review is dedicated to professors Alexey Morachevsky and Natalia Smirnova to celebrate their distinguished contributions to research and education at the University of St.Petersburg.

References

1. *Weissberger A., Rossiter B. W.* Physical methods of chemistry. New York: Wiley-Interscience, 1971.

2. *Wilhelm E., Battino R.* Precision methods for the determination of the solubility of gases in liquids // CRC Critical Reviews in Analytical Chemistry. 1985. Vol. 16. P. 129–175.

3. *Wilhelm E., Battino R., Wilcock R. J.* Low-pressure solubility of gases in liquid water // Chem. Rev. 1977. Vol. 77. P. 219–262.

4. Measurement of the thermodynamic properties of multiple phases / eds R. D. Weir, T. W. de Loos. [W. p.]: IUPAC Commission on Thermodynamics-Elsevier Science, 2005. (Experimental Thermodynamics. Vol. VII.)

5. *Richon D.* Elements de thermodynamique experimentale (Cours de Thermodynamique CB 302, 2242). Ecole des Mines de Paris (Unpublished), 1997.

6. *Richon D.* New experimental developments for phase equilibrium measurements // Fluid Phase Equilibria. 1996. Vol. 116. P. 421–428.

7. *Raal J. D., Mühlbauer A. L.* Phase equilibria: measurement and computation. [W. p.]: CRC, 1997.

8. *Malanowski S.* Experimental methods for vapour-liquid equilibria. Part I. Circulation methods // Fluid Phase Equilibria. 1982. Vol. 8. P. 197–219.

9. *Malanowski S.* Experimental methods for vapour-liquid equilibria. Part II. Dew- and bubble-point method // Fluid Phase Equilibria. 1982. Vol. 9. P. 311–317.

10. *Hala E., Pick J., Fried V., Vilim O.* Vapour-liquid equilibrium: 2nd ed. Oxford: Pergamon Press, 1967.

11. *Dohrn R., Brunner G.* High-pressure fluid-phase equilibria: Experimental methods and systems investigated (1988–1993) // Fluid Phase Equilibria. 1995. Vol. 106. P. 213–282.

12. *Maloney D. P., Prausnitz J. M.* Solubility of ethylene in liquid, low-density polyethylene at industrial-separation pressures // Ind. Eng. Chem. Proc. Des. Dev. 1976. Vol. 15. P. 216–220.

13. *Liu D. D., Prausnitz J. M.* Solubilities of gases and volatile liquids in polyethylene and in ethylene-vinyl acetate copolymers in the region 125–225 °C // Industrial Engineering Chemistry Fundamentals. 1976. Vol. 15. P. 330–335.

14. *Rosenboom J.-G., Afzal W., Prausnitz J. M.* Solubilities of some organic solutes in 1-ethyl-3-methylimidazolium acetate. Chromatographic measurements and predictions from COSMO-RS // J. Chem. Thermodynamics. 2012. Vol. 47. P. 320–327.

15. *Heintz A., Lichtenthaler R. N., Prausnitz J. M.* Solubilities of volatile solvents in polyvinyl acetate, polyvinyl chloride, and their random copolymers // Berichte der Bunsengesellschaft für physikalische Chemie. 1979. Vol. 83. P. 926–928.

16. *Lichtenthaler R. N., Liu D. D., Prausnitz J. M.* Polymer-solvent interactions from gas-liquid chromatography with capillary columns // Macromolecules. 1974. Vol. 7. P. 565–570.

17. *Heintz A., Kulikov D. V., Verevkin S. P.* Thermodynamic properties of mixtures containing ionic liquids. 1. Activity coefficients at infinite dilution of alkanes, alkenes, and alkylbenzenes in 4-methyl-n-butylpyridinium tetrafluoroborate using gas-liquid chromatography // J. Chem. Eng. Data. 2001. Vol. 46. P. 1526–1529.

18. *Cruickshank A. J. B., Windsor M. L., Young C. L.* The use of gas-liquid chromatography to determine activity coefficients and second virial coefficients of mixtures. ii. Experimental studies on hydrocarbon solutes // Proc. Royal Soc. of London. Series A: Mathematical and Physical Sciences. 1966. Vol. 295. P. 271–287.

19. *Jennings W.* Gas chromatography with glass capillary columns. New York: Academic Press, 1980.

20. *Ettre L. S.* Open tubular columns in gas chromatography. New York: Plenum Press, 1965.

21. *Handley A. J., Adlard E. R.* Gas chromatographic techniques and applications. Sheffield: Academic Press, 2001.

22. *Grob R. L., Barry E. F.* Modern practice of gas chromatography. Hoboken, NJ: Wiley-Interscience, 2004.

23. *Yoo B., Afzal W., Prausnitz J. M.* Henry's constants and activity coefficients of some organic solutes in 1-butyl,3-methylimidazolium hydrogen sulfate and in 1-methyl,3-trimethylsilylmethylimidazolium chloride // J. Chem. Thermodynamics. 2013. Vol. 57. P. 178–181.

24. *Leroi J., Masson J., Renon H.* et al. Accurate measurement of activity coefficient at infinite dilution by inert gas stripping and gas chromatography // Ind. Eng. Chem. Proc. Des. Dev. 1977. Vol. 16. P. 139–144.

25. *Richon D., Antoine P., Renon H.* Infinite dilution activity coefficients of linear and branched alkanes from C1 to C9 in n-hexadecane by inert gas stripping // Ind. Eng. Chem. Proc. Des. Dev. 1980. Vol. 19. P. 144–147.

26. *Richon D., Renon H.* Infinite dilution Henry's constants of light hydrocarbons in n-hexadecane, n-octadecane, and 2,2,4,4,6,8,8-heptamethylnonane by inert gas stripping // J. Chem. Eng. Data. 1980. Vol. 25. P. 59–60.

27. *Richon D., Sorrentino F., Voilley A.* Infinite dilution activity coefficients by the inert gas stripping method: extension to the study of viscous and foaming mixtures // Ind. Eng. Chem. Proc. Des. Dev. 1985. Vol. 24. P. 1160–1165.

28. *Kojima K., Zhang S., Hiaki T.* Measuring methods of infinite dilution activity coefficients and a database for systems including water // Fluid Phase Equilibria. 1997. Vol. 131. P. 145–179.

29. *Eckert C. A., Sherman S. R.* Measurement and prediction of limiting activity coefficients // Fluid Phase Equilibria. 1996. Vol. 116. P. 333–342.

30. *Coquelet C., Richon D.* Measurement of Henry's law constants and infinite dilution activity coefficients of propyl mercaptan, butyl mercaptan, and dimethyl sulfide in methyldiethanolamine

(1) + water (2) with $w_1 = 0.50$ using a gas stripping technique // J. Chem. Eng. Data. 2005. Vol. 50. P. 2053–2057.

31. *Duhem P., Vidal J.* Extension of the dilutor method to measurement of high activity coefficients at infinite dilution // Fluid Phase Equilibria. 1978. Vol. 2. P. 231–235.

32. *Afzal W., Yoo B., Prausnitz J. M.* Inert-gas-stripping method for measuring solubilities of sparingly soluble gases in liquids. Solubilities of some gases in protic ionic liquid 1-butyl, 3-hydrogenimidazolium acetate // Industrial & Engineering Chemistry Research. 2012. Vol. 51. P. 4433–4439.

33. *Richon D.* New equipment and new technique for measuring activity coefficients and Henry's constants at infinite dilution // Review of Scientific Instruments. 2011. Vol. 82. 025108.

34. *Afzal W., Breil M. P., Théveneau P.* et al. Phase equilibria of mixtures containing glycol and n-alkane: experimental study of infinite dilution activity coefficients and modeling using the Cubic-Plus-Association Eq. of State // Industrial & Engineering Chemistry Research. 2009. Vol. 48. P. 11202–11210.

35. *Gupta R. B., Prausnitz J. M.* Vapor-liquid equilibria of copolymer + solvent and homopolymer + solvent binaries: New experimental data and their correlation // J. Chem. Eng. Data. 1995. Vol. 40. P. 784–791.

36. *Rodríguez O., Fornasiero F., Arce A.* et al. Solubilities and diffusivities of water vapor in poly(methylmethacrylate), poly (2-hydroxyethylmethacrylate), poly(N-vinyl-2-pyrrolidone) and poly (acrylonitrile) // Polymer. 2003. Vol. 44. P. 6323–6333.

37. *Bonner D. C., Prausnitz J. M.* Thermodynamic properties of some concentrated polymer solutions // J. Polymer Sci.: Polymer Physics Edition. 2003. Vol. 12. P. 51–73.

38. *Arce A., Fornasiero F., Rodríguez O.* et al. Sorption and transport of water vapor in thin polymer films at 35 ℃ // Phys. Chem. Chem. Phys. 2003. Vol. 6. P. 103–108.

39. *Anthony J. L., Maginn E. J., Brennecke J. F.* Solubilities and thermodynamic properties of gases in the ionic liquid 1-n-butyl-3-methylimidazolium hexafluorophosphate // J. Phys. Chem. (B). 2002. Vol. 106. P. 7315–7320.

40. *Panayiotou C., Vera J. H.* Thermodynamics of polymer-polymer-solvent and block copolymer-solvent systems. I: Experimental measurements // Polymer J. 1984. Vol. 16. P. 89–102.

41. *Afzal W., Prausnitz J. M.* Solubilities of some gases in three imidazolium-based ionic liquids // submitted to J. Chem. Thermodynamics.

42. *Afzal W., Breil M. P., Mohammadi A. H.* et al. Estimation of the impact of sulfur species on glycol dehydration // Proc. VIII IberoAmerican Conf. on Phase Equilibria and Fluid Properties for Process Design — EQUIFASE. 2009.

43. *Afzal W., Breil M. P., Tsivintzelis I.* et al. Experimental study and phase equilibrium modeling of systems containing acid gas and glycol // Fluid Phase Equilibria. 2012. Vol. 318. P. 40–50.

44. *Afzal W.* Phase equilibria of glycol-natural gas systems. PhD thesis. Paris, 2009.

45. *Jacquemin J., Costa Gomes M. F., Husson P., Majer V.* Solubility of carbon dioxide, ethane, methane, oxygen, nitrogen, hydrogen, argon, and carbon monoxide in 1-butyl-3-methylimidazolium tetrafluoroborate between temperatures 283 and 343 K and at pressures close to atmospheric // J. Chem. Thermodynamics. 2006. Vol. 38. P. 490–502.

46. *Fontalba F., Richon D., Renon H.* Simultaneous determination of vapor-liquid equilibria and saturated densities up to 45 MPa and 433 K // Rev. Scientific Instruments. 1984. Vol. 55. P. 944–951.

47. *Gibbs R. E., Van Ness H. C.* Vapor-liquid equilibria from total-pressure measurements. A new apparatus // Industrial and Engineering Chemistry Fundamentals. 1972. Vol. 11. P. 410–413.

48. *Fischer K., Wilken M.* Experimental determination of oxygen and nitrogen solubility in organic solvents up to 10 MPa at temperatures between 298 K and 398 K // J. Chem. Thermodynamics. 2001. Vol. 33. P. 1285–1308.

49. *Fischer K., Gmehling J.* P-x and $\gamma\infty$ data for the different binary butanol-water systems at 50 °C // J. Chem. Eng. Data. 1994. Vol. 39. P. 309–315.

Статья поступила в редакцию 8 октября 2012 г.